



Alkyl group-tagged ruthenium indenylidene complexes: Synthesis, characterization and metathesis activity



Baoyi Yu ^b, Fatma B. Hamad ^d, Karen Leus ^b, Alex A. Lyapkova ^c, Kristof Van Hecke ^b, Francis Verpoort ^{a,b,c,*}

^a Laboratory of Organometallics, Catalysis and Ordered Materials, State Key Laboratory of Advanced Technology for Materials Synthesis and Processing, School of Chemistry, Chemical Engineering and Life Sciences, Wuhan University of Technology, Wuhan 430070, PR China

^b Department of Inorganic and Physical Chemistry, Ghent University, Krijgslaan 281-S3, 9000 Ghent, Belgium

^c National Research Tomsk Polytechnic University, Tomsk, Russian Federation

^d Dar es Salaam University College of Education, Faculty of Science, Department of Chemistry, P.O. Box 2329, Dar es Salaam, Tanzania

ARTICLE INFO

Article history:

Received 1 March 2015

Received in revised form

14 April 2015

Accepted 28 April 2015

Available online 2 June 2015

Keywords:

Olefin metathesis

Ruthenium

Indenylidene

Homogeneous

Catalysis

ABSTRACT

We report on the synthesis of ruthenium indenylidene catalysts $[\text{RuCl}_2(3-\text{R}-1\text{-indenylidene})(\text{PCy}_3)_2]$ in which R is iso-propyl (**7a**), tert-butyl (**7b**) or cyclohexyl (**7c**). The obtained alkyl tagged indenylidene catalysts were analyzed by means of IR, elemental analysis, NMR and single crystal X-Ray diffraction analysis. Furthermore, the catalytic performance of these new complexes was examined in different metathesis reactions: ring-closing metathesis (RCM), ring-closing ene-yne metathesis (RCEYM), ring-opening metathesis polymerization (ROMP) and cross metathesis (CM), exhibiting a comparable activity in comparison with the commercially available catalyst **3a**.

© 2015 Elsevier B.V. All rights reserved.

1. Introduction

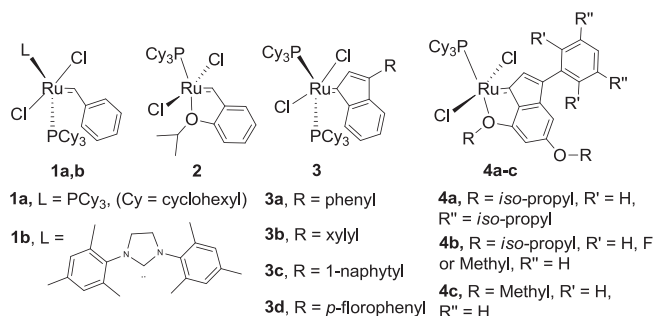
Olefin metathesis as a powerful synthesis tool plays an important role in synthetic chemistry [1]. The suitability of ruthenium based olefin metathesis catalysts over other transition metals is based on their ability to combine both high activity and excellent stability [2]. Since the discovery of the 1st generation ruthenium benzylidene catalyst **1a** (Fig. 1) by Grubbs and coworkers [3], the great focus of metathesis pioneers has been on the development of new catalysts with enhanced catalytic performance. A notable development was the substitution of one of the labile phosphines by *N*-heterocyclic carbenes (NHC), which resulted in the more stable 2nd generation catalyst **1b** [4]. Another important contribution in this area was the development of the chelating benzylidene Grubbs-Hoveyda type catalyst **2**, which showed an increased stability in comparison to complex **1a** [5]. Besides ruthenium benzylidene catalysts **1** and **2**, the ruthenium indenylidene

catalysts have also been well-studied, for example complex **3a** [6]. The peculiar attribution of ruthenium indenylidene catalysts is their ease of synthesis [7], and increased stability under harsh conditions. Additionally, they exhibit a comparable (or sometimes higher) catalytic performance than their benzylidene counterparts [7a,8]. Furthermore, the ruthenium indenylidene catalysts were often employed as starting materials for the synthesis of other families of ruthenium catalysts, e.g. benzylidene [9] or ether chelating benzylidene catalysts [10].

The ease of synthesis and high catalytic performance of ruthenium indenylidene catalysts have encouraged some researchers to modify these basic indenylidene structures. In 2010, the catalyst **4a**, bearing the bidentate iso-propoxyindenylidene ligand, was reported by Bruneau's group which was an analogue of complex **2**. Although a lower catalytic initiation speed was observed, the reported complex showed improved thermal stability in comparison with its benzylidene analogue **2** [11]. Later on, substituted variants with the general structure of **4b** of the chelating indenylidene complexes were reported by the same group [12]. Moreover, Schrödi et al. reported on the *in-situ* generated methoxy coordinated bidentate indenylidene catalyst **4c**, which showed a comparable activity to complex **2** [13]. Recently, we have reported the

* Corresponding author. Department of Inorganic and Physical Chemistry, Ghent University, Krijgslaan 281-S3, 9000 Ghent, Belgium.

E-mail address: Francis.verpoort@ugent.be (F. Verpoort).



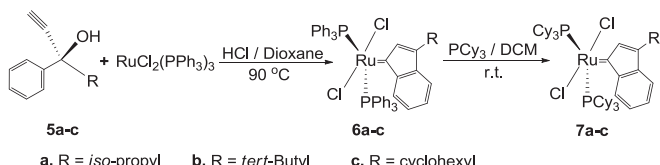
synthesis of first generation ruthenium indenylidene complexes **3b-d** featuring a functionalized 3-phenyl group based on the general scaffold of complex **3a**, the resulting complexes showed comparable catalytic activity relative to the reference catalyst **3a** [14].

So far, all the reported ruthenium indenylidene catalysts were derived from 1,1-diaryl-propargylic alcohols [11–13,15]. Nevertheless, only one of the two aryl groups is necessary to be involved in the indenylidene formation process. Some attempts for obtaining ruthenium indenylidene complexes from a mono aryl propargylic alcohol were not successful [13b,16]. Herein, we report on the successful synthesis of ruthenium indenylidene catalysts employing a library of 1-alkyl-1-phenyl-2-propyn-1-ol ligands. The characterization and catalytic activity of the obtained first generation single species with the general structure of $\text{RuCl}_2(3\text{-alkyl-1-indenylidene})(\text{PCy}_3)_2$ are described.

2. Results and discussion

A convenient way to obtain a ruthenium based alkylidene catalyst (vinylidene [17], allenylidene [6c,18] and indenylidene [7a,12,19]) is the direct treatment of non-hazardous propargylic alcohols with $\text{RuCl}_2(\text{PPh}_3)_3$ [20]. However, the ruthenium indenylidene catalysts were generally preferred among these three families since they showed a relatively more active performance in olefin metathesis reactions in comparison to their vinylidene or allenylidene analogues [15b]. Especially, the latter two catalysts types could be decomposed by H_2O [21] or O_2 , [22] consequently, the cleavage of the $\text{C}_\alpha = \text{C}_\beta$ bond resulted in a formation of a CO ligand. Thus, in terms of catalyst efficiency and hence the cost effectiveness of the expensive ruthenium used, ruthenium indenylidene catalysts are more preferred [15b,20c,f]. The indenylidene precursor complex **3a** could be obtained from a well-established general strategy, which involves the reaction of $\text{RuCl}_2(\text{PPh}_3)_3$ and 1,1-diphenyl-2-propyn-1-ol in THF/dioxane in presence of acid and followed by an exchange of PPh_3 with PCy_3 [7b].

The propargylic alcohols **5a** [23], **5b** [24] and **5c** [25] (Scheme 1) were prepared by direct addition of ethynylmagnesium bromide to the relative keton in THF and were purified by column chromatography. Subsequently, **5a-c** were allowed to react with $\text{RuCl}_2(\text{PPh}_3)_3$ in dioxane in the presence of HCl at 90 °C [26]. The



Scheme 1. Synthesis of complexes **7a-c** from **5a-c**.

reactions yielding complexes **6a-c** were monitored by ^{31}P NMR spectroscopy. The reaction solutions all showed a dark red color after 10 min and according to the ^{31}P NMR spectra the reactions were finished. Single phosphine peaks for each compound were observed at 29.6 ppm for **6a**, 29.1 ppm for **6b** and 29.5 ppm for **6c** from the ^{31}P NMR spectra (see Fig. S.4,6,8), after purification by simply washing with *n*-hexane and methanol. The structural configurations of **6a-c** were confirmed by single crystal X-ray analysis (see the section “Single crystal X-ray diffraction analysis”). Later on, complexes **7a-c** were obtained by the exchange of the PPh_3 on **6a-c** by PCy_3 in dichloromethane (Scheme 1) as reddish brown solids in high yield (91–95%) after washing with *n*-pentane. The purities of the obtained complexes **7a-c** were analyzed by elemental analysis. The characterization of **7a-c** was done by means of IR, NMR and single crystal X-ray diffraction (see the section “Single crystal X-ray diffraction analysis”). For the NMR data, assignment of each proton and carbon resonance of the ^1H - (see Fig. S.9,12,15) and $^{13}\text{C}\{^1\text{H}\}$ (see Fig. S.10,13,16) NMR spectra was achieved by a combination of the 1D and 2D ($^1\text{H}\{^1\text{H}\}$ COSY, $^1\text{H}\{^{13}\text{C}\}$ HSQC and HMBC) NMR data (see the section of “Structure elucidation of NMR spectral data” in the ESI).

2.1. Single crystal X-ray diffraction analysis

Crystallization of **6a-c** was carried out by incubation of reaction solutions at room temperature for two days affording crystals, suitable for X-ray structure determination. Their structures are shown in Fig. 2.

Compounds **6a** and **6c** crystallized both in the centro-symmetric triclinic space group *P*-1, while compound **6b** crystallized in the centro-symmetric monoclinic space group *I*2/a. The asymmetric unit of the structures consists of one ruthenium complex molecule and additional dioxane solvent molecules (one dioxane molecule for **6a**, two-and-a-half for **6b** and three for **6c**). For **6a**, the 3-*iso*-propyl-1-indenylidene moiety is completely disordered over two

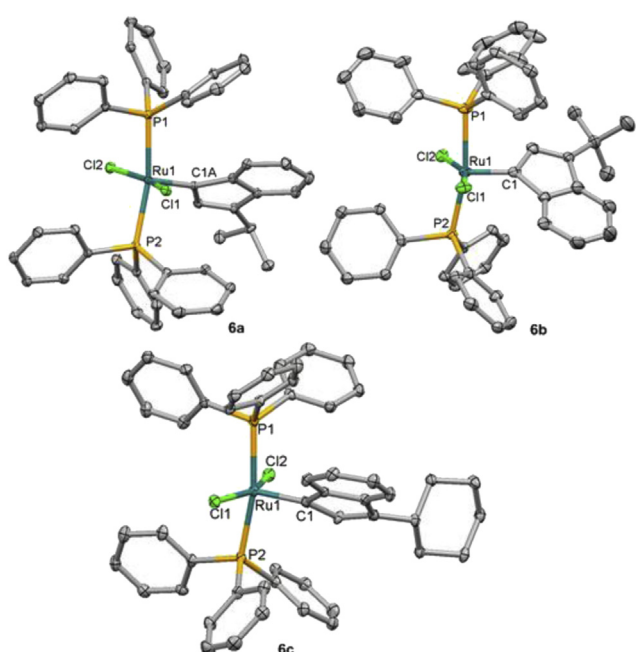


Fig. 2. ORTEP representations of the structures of complexes **6a-c** (thermal ellipsoids are shown at the 30% probability level), showing the atom labeling scheme of the heteroatoms and carbon atom C1 and C1A. Hydrogen atoms and dioxane solvent molecules are omitted for clarity. For **6a**, the disorder of the 3-*iso*-propyl-1-indenylidene moiety is omitted for clarity.

positions, turned over about 175.8° with respect to each other. Complexes **6a–c** feature a slightly distorted square-pyramidal geometry around the ruthenium atom, similar to complexes **1a** [27] and **3a** [28], with the indenyldiene moieties in the axial position. The Ru=C bond lengths for **6a** and **6c** are 1.861(6)/1.85(3) and 1.869(5) Å, respectively, while these values are slightly longer than the one for **6b** (1.833(8) Å) (Table 1). The Ru–Cl bond lengths for **6a–c** are found between 2.345(1) and 2.375(1) Å and Ru–P bond lengths range from 2.370(2) to 2.400(2) Å. P–Ru–P and Cl–Ru–Cl angles for these three species are within $166\text{--}169^\circ$ and $158\text{--}160^\circ$, respectively.

Crystals, suitable for X-ray diffraction analysis, of **7a-c** were grown from a fast evaporation (a few seconds) of a dichloromethane solution of complexes on a glass slide. Their structures are shown in Fig. 3.

Apparently, all complexes **7a-c** crystallized in the *R*-3 trigonal space group with one ruthenium complex in the asymmetric unit. Similar to **1a** [27], **3a** [28] and **6a-c**, a square-pyramidal geometry around the ruthenium center is observed for **7a-c**. Some selected structural data of complexes **7a-c** are listed in Table 1, in comparison with complex **1a** and the parent complex **3a**. Complexes **7a-c** exhibit Ru=C bond lengths of 1.869(5), 1.858(8) and 1.860(6) Å, respectively, while complex **1a** and **3a** show Ru=C bond lengths of 1.841(2) Å and 1.882(6) Å, respectively. The bond distances of Ru–Cl are quite similar for **1a**, **3a** and **7a-c**, and are all in the range of 2.385(2)–2.408(2) Å. Considering the Ru–P bond lengths, all the bond lengths are between 2.4030(7) and 2.427(2) Å for all the species **1a**, **3a** and **7a-c**. The Cl–Ru–Cl angles for the new species and **3a** can be summarized in a value of 164° without significant differences, while the angle is 167° for **1a**, which is obviously larger than the ones for the former indenylidene complexes. **7a-c** show P–Ru–P bond angles of 161° in comparison with **1a** and **3a** (162° and 159°, respectively). Potential intramolecular hydrogen bonds are observed between the indenylidene ligand and the chlorides for **7a-c**: C2–H2···Cl2 and C7–H7···Cl1 (C···Cl distance of 3.19–3.25 Å) (number scheme see Fig. S.1).

2.2. Catalytic activity studying in olefin metathesis reactions

The catalytic performance of the new complexes **7a–c** was tested in some well-established model olefin metathesis reactions [7a,29]. More specifically, in the ring-closing metathesis (RCM) of diethyl 2,2-diallylmalonate (**8**) (Scheme 2, a), the ring-opening metathesis polymerization (ROMP) of *cis,cis*-cycloocta-1,5-diene (COD) (Scheme 2, b), the ring-closing ene-yne metathesis (RCEY) of (1-(allyloxy)prop-2-yne-1,1-diy)dibenzene (**9**) (Scheme 2, c) and the cross metathesis (CM) between allylbenzene and *cis*-1,4-diacetoxy-2-butene (Scheme 2, d). The results of all the catalytic tests are depicted in Figs. 4–7.

Fig. 4 displays the catalytic performance of **7a–c** in comparison with **1a** and **3a** for the RCM of **8** (**Scheme 2**, a). A catalyst loading of 0.5 mol% was applied at 20 °C in CDCl₃. All the new complexes **7a–c**

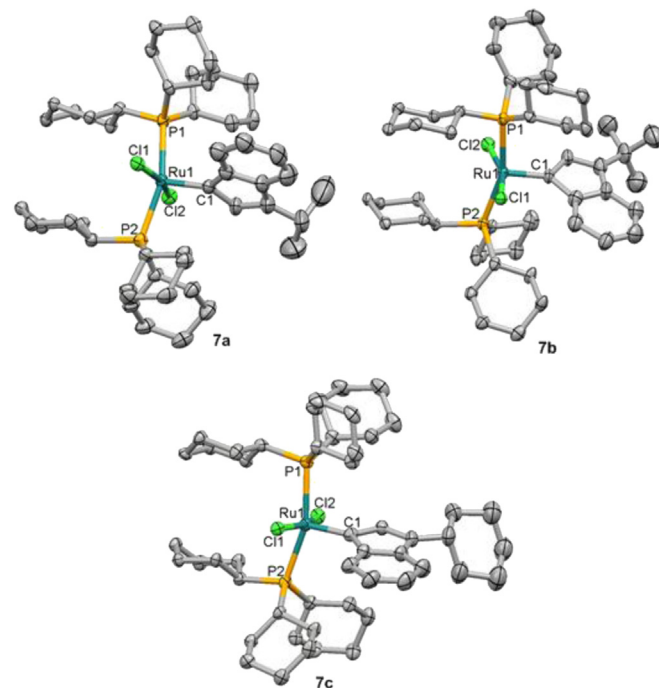
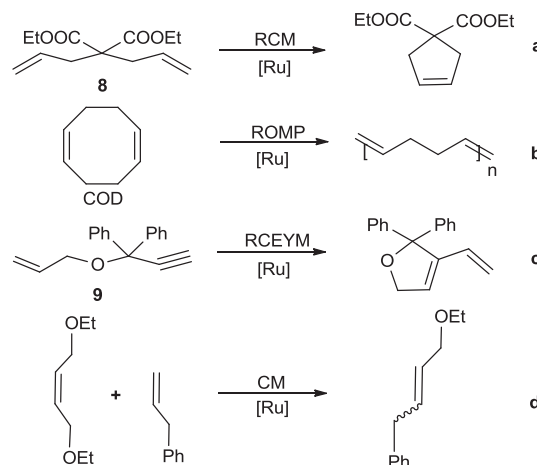


Fig. 3. ORTEP representations of the structures of complexes **7a–c** (thermal ellipsoids are shown at the 30% probability level), showing the atom labeling scheme of the heteroatoms and carbon atom C1. Hydrogen atoms are omitted for clarity.



Scheme 2. Olefin metathesis model reactions **a**, **b**, **c**, **d**.

as well as **3a** showed a similar conversion pattern and a similar kinetics. After approximately 30 min of reaction, complexes **7b** and **7c** exhibited a conversion of 93% whereas for complex **7a**, a conversion of 90% was noted, which was comparable to the catalytic

Table 1

Selected bond lengths (\AA) and angles ($^\circ$) for complexes **6a-c** and **7a-c** in comparison with **1a** and **3a**.

	6a	6b	6c	1a^a	3a^b	7a	7b	7c
Ru=C	1.861(6)/1.85(3)	1.833(8)	1.869(5)	1.841(2)	1.882(6)	1.869(5)	1.858(8)	1.860(6)
Ru-Cl	2.3577(7)	2.367(2)	2.345(1)	2.3949(6)	2.389(2)	2.392(1)	2.393(2)	2.389(2)
	2.3686(7)	2.362(2)	2.374(1)	2.3957(6)	2.408(2)	2.389(1)	2.385(2)	2.395(2)
Ru-P1	2.3776(9)	2.375(2)	2.396(1)	2.4030(7)	2.427(2)	2.414(2)	2.416(2)	2.419(2)
Ru-P2	2.395(1)	2.400(2)	2.370(2)	2.4066(7)	2.416(2)	2.416(2)	2.413(1)	2.418(2)
P-Ru-P	165.99(3)	168.01(8)	169.00(5)	162.22(2)	159.03(7)	160.69(6)	160.92(7)	160.63(7)
Cl-Ru-Cl	160.10(3)	157.52(8)	158.35(5)	166.87(2)	163.91(7)	163.88(6)	163.84(7)	164.06(7)

^a Data according to reference [27]

^b Data according to reference [28]

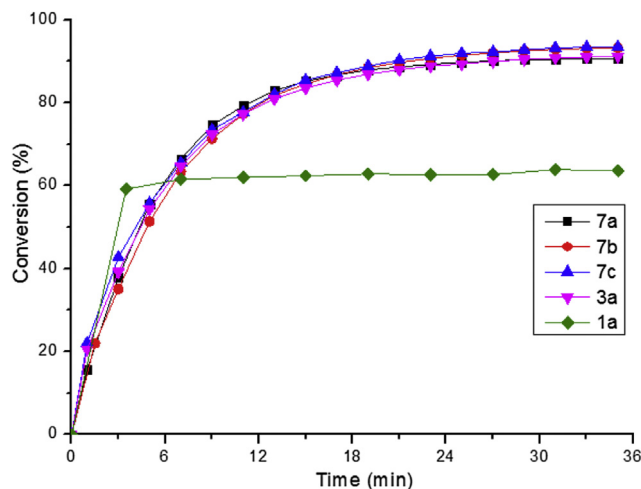


Fig. 4. RCM of **8** (Scheme 2a) with complexes **1a**, **3a** and **7a-c** (0.5 mol%) at 20 °C in CDCl_3 . Lines are intended as visual aid.

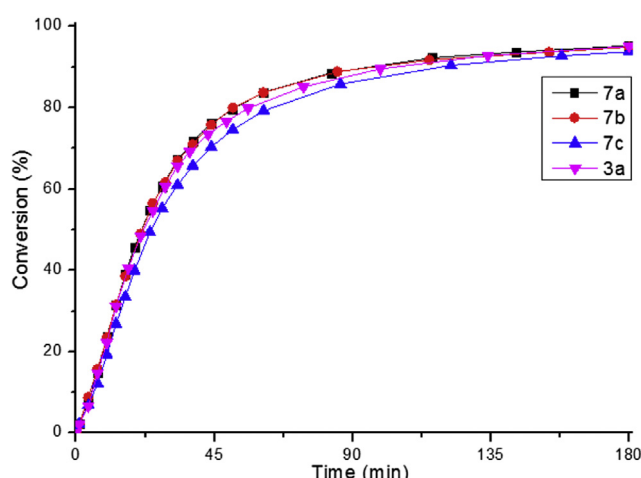


Fig. 5. ROMP of COD (Scheme 2, b) with complexes **3a** and **7a-c** (0.033 mol%) at 25 °C in CDCl_3 . Lines are intended as visual aid.

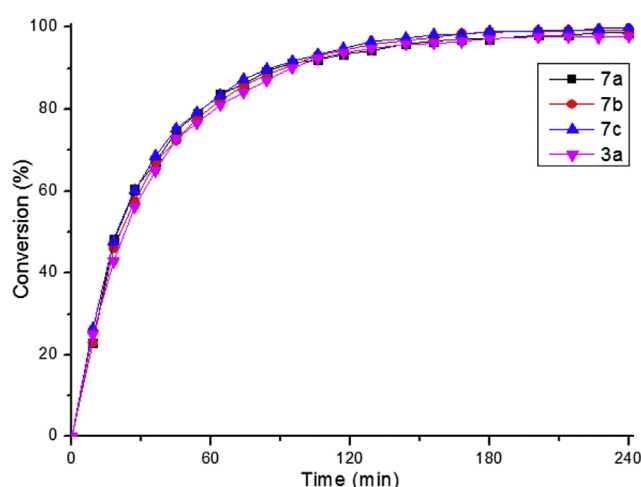


Fig. 6. RCEYM of **9** (Scheme 2, c) with complexes **3a** and **7a-c** (5 mol%) at 50 °C in toluene. Lines are intended as visual aid.

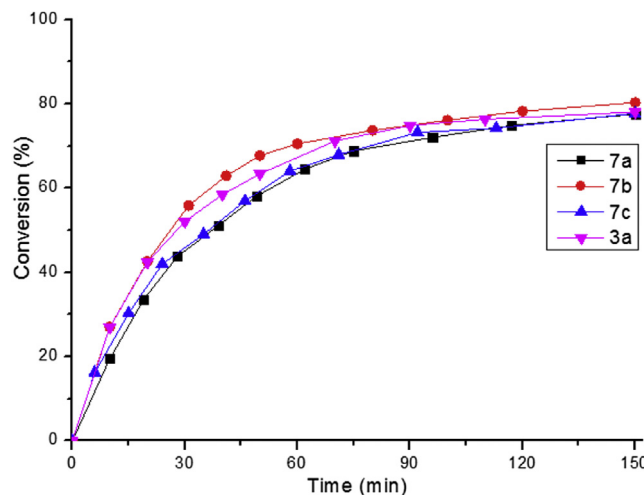


Fig. 7. CM between allylbenzene and *cis*-1,4-diacetoxy-2-butene (Scheme 2, d) applying catalyst loading of 2.5 mol% at 25 °C in dichloromethane. Lines are intended as visual aid.

performance of the reference complex **3a**. In contrast, the first generation Grubbs catalyst **1a** exhibited a faster initiation while a much lower conversion was observed (about 62%) in comparison to its indenylidene analogues [29].

The conversion patterns for the ROMP of COD (Scheme 2, b) using catalysts **3a** and **7a-c** are depicted in Fig. 5. The catalytic performance of complex **3a** in the ROMP of COD was in agreement with previous report [30]. Moreover, as can be seen from Fig. 5, all the new species showed a similar catalytic efficiency as the reference complex **3a**. No significant difference can be observed among all the employed complexes **3a** and **7a-c** in any stage of the reaction.

Furthermore, all the synthesized complexes were examined in the RCEYM of substrate **9** (Scheme 2, c) and the CM between allylbenzene and *cis*-1,4-diacetoxy-2-butene (Scheme 2, d). Also in the latter two catalytic tests, the novel catalysts exhibited a similar metathesis activity as the benchmark catalyst **3a** (Figs. 6 and 7).

All these indenylidene complexes **3a** and **7a-c** showed a similar catalytic performance in all the investigated olefin metathesis reactions, however, they showed a better overall performance than the Grubbs first generation catalyst **1a** in the RCM reaction of substrate **8**.

The effect of a modification of the alkylidene moieties on the catalytic activities could be either via electronic influences [31] on the ruthenium center or via steric repulsion between the surrounding ligands [32]. In our case, we believe that the indenylidene fragment, between the ruthenium center and the modified sites, suppresses the electronic effect from the phenyl (**3a**) or alkyl (**7a-c**) groups.

Considering the steric aspect, it was reported that the interaction between a bulkier NHC and indenylidene ligands could stimulate the dissociation of PCy_3 , therefore resulting in a high initiation rate of the ruthenium indenylidene catalyst [32]. In comparison with second generation type catalysts, the dissociation rate of PCy_3 of first generation type catalysts is relatively faster [33]. As a matter of fact, the reaction rate of first generation type catalysts is not dependent on the dissociation of PCy_3 , in other words, the dissociation of phosphine is not the rate determining step for first generation catalysts, which was revealed by Grubbs group [33a]. Therefore, the function of steric stimulation to release the PCy_3 group to achieve faster catalysts initiation for a first generation type catalyst was reduced. Especially, in our study, as can be seen from

Table 1, most of the bond lengths and bond angles in complexes **7a–c** are similar to these in complex **3a**, no significant steric interaction was noted between the investigated modified parts (3-alkyl groups) and any of the two PCy₃ groups. So, we believe that the similarity of the catalytic performance of the investigated indenylidene catalysts is probably due to the resemblance of their configuration around the ruthenium center.

3. Conclusions

The current work extends the scope of ligands, which can be employed to generate ruthenium indenylidene catalysts from the previous reported 1,1-diaryl-propargylic alcohols to the 1-alkyl-1-phenylpropargylic alcohols. A new library of ruthenium indenylidene complexes has been synthesized successfully and has been characterized by means of IR, elemental analysis, NMR and single crystal X-ray diffraction. The X-ray diffraction data demonstrate that all complexes exhibiting quite similar values for both the bond lengths and angles of these ligands around the ruthenium center. Moreover, the catalytic activity of these complexes was examined in various model olefin metathesis reactions. As a result, no significant difference in catalytic performance was observed among the new catalysts themselves nor between the new catalysts and the reference catalyst **3a**. The changes in the geometry from the phenyl group (**3a**) by the alkyl groups (**7a–c**) showed negligible effect on the catalytic activity on these first generation ruthenium indenylidene complexes.

4. Experimental section

4.1. General consideration

All the reactions were carried out under argon atmosphere. Solvents were dried and freshly distilled prior to use. For drying dichloromethane, CaH₂ was used as drying agent whereas for toluene, *n*-hexane, *n*-pentane and 1,4-dioxane, sodium was employed as drying agent and benzophenone was used as indicator. The compounds RuCl₂(PPh₃)₃ [34], 4-methyl-3-phenyl-1-pentyn-3-ol [23], 4,4-dimethyl-3-phenyl-1-pentyn-3-ol [24], 1-cyclohexyl-1-phenyl-2-propyn-1-ol [25] and (1-(allyloxy)prop-2-yne-1,1-diyl)dibenzene [35] were prepared according to the literature. *n*-Hexane, *n*-pentane, 1,4-dioxane and toluene were purchased from Fiers. Diethyl 2,2-diallylmalonate, HCl in 1,4-dioxane (1M), benzophenone, *cis,cis*-octa-1,5-diene and allylbenzene were bought from Aldrich. *cis*-1,4-diacetoxy-2-butene was obtained from ABCR.

The 1D and 2D NMR spectra were recorded on Bruker Avance 300 MHz and 500 MHz spectrometers. Chemical shifts were listed in ppm using tetramethylsilane with residual solvent resonance as an internal standard (¹H, ¹³C) or external standard H₃PO₄ (³¹P). The exact indicated number of each assigned proton and carbon of the new complexes could be found from Fig. S.1 in the supporting information. Elemental analyses were performed on a CHNS-0 Analyzer from Interscience. Gas chromatography measurements were carried out on a Agilent 7890A instrument equipped with a flame ionization detector and an HP-5 5% phenyl methyl siloxane column (DB-5, column length: 30 m, inside diameter: 0.25 mm, outside diameter: 0.32 mm, film thickness: 0.25 mm). X-ray diffraction data were collected on an Agilent Supernova Dual Source (Cu at zero) diffractometer equipped with an Atlas CCD detector using CuK α radiation ($\lambda = 1.54178 \text{ \AA}$) and ω scans. All images were interpreted and integrated with the program CrysAlisPro (Agilent Technologies) [36]. Using Olex2 [37], the structures were solved by direct methods using the ShelXS structure solution program [38] and refined by full-matrix least-squares on F² using

the ShelXL program [39]. Non-hydrogen atoms were anisotropically refined and the hydrogen atoms in the riding mode and isotropic temperature factors fixed at 1.2 times U(eq) of the parent atoms (1.5 times for methyl groups). CCDC-1032813–1032818 contain the Supplementary crystallographic data for this paper. These data can be obtained free of charge from The Cambridge Crystallographic Data Centre via www.ccdc.cam.ac.uk/data_request/cif.

Structure elucidation of NMR spectral data of **7a–c**. Standard benchmark screening procedures were done following the literature and applied details as well as NMR spectra of **6a–c** and **7a–c** were also listed in the Supporting information.

4.2. General synthesis condition for the ruthenium complexes **6a–c** and **7a–c**

The RuCl₂(PPh₃)₃ (1 eq., 0.50 mmol) was added to the propargylic alcohols **5** (1.3 eq., 0.65 mmol) in 5 mL HCl/dioxane solution (0.1 mol/L). The reaction mixture was heat up in an oil bath at 90 °C and was monitored by ³¹P NMR. The reaction was completed after only 10 min of reaction. Afterwards, all the volatiles were removed under vacuum and hexane (20 mL) was added. The flask was placed in an ultrasonic bath until the solid was homogenously distributed. The resulting suspension was filtered and washed with *n*-hexane and methanol affording a red-brown powder. The products **6** were measured by ¹H and ³¹P NMR spectroscopy. Single crystal of **6** suitable for X-ray diffraction analysis was obtained by incubation of the reaction solution at room temperature for two days.

In a second step, the obtained ruthenium complex **6** was mixed with tricyclohexylphosphine (3.0 eq., 1.5 mmol) in dry dichloromethane (10 mL) under argon atmosphere and vigorously stirred at room temperature. The reaction was monitored by ³¹P NMR. After completion of the reaction (about 3 h), the resulting slurry was dried under vacuum and cold *n*-pentane (5 mL) was added. Filtration afforded a red-brown powder, which was afterwards washed with cold *n*-pentane (2 x 5 mL) and drying under vacuum affording the reddish brown powder **7**. Single crystal of **7** suitable for X-ray diffraction analysis was grown from a fast evaporation of the complex dichloromethane solution on a glass slide.

4.2.1. RuCl₂(3-iso-propyl-1-indenylidene)(PPh₃)₂, **6a**

¹H NMR (300 MHz, CDCl₃, 20 °C, TMS): δ 7.48–7.54 (m, 12H), 7.38 (t, ³J_{H,H} = 7.4 Hz, 6H), 7.27 (t, ³J_{H,H} = 7.5 Hz, 12H), 7.21 (t, ³J_{H,H} = 7.4 Hz, 1H), 6.95 (d, ³J_{H,H} = 7.2 Hz, 1H), 6.86 (d, ³J_{H,H} = 7.2 Hz, 1H), 6.53 (t, ³J_{H,H} = 7.4 Hz, 1H), 6.17 (s, 1H), 2.09 (sept, ³J_{H,H} = 6.6 Hz, 1H), 1.01 (d, ³J_{H,H} = 6.8 Hz, 6H); ³¹P{¹H}NMR (121 MHz, CDCl₃, 20 °C): δ 29.6 (s); elemental analysis calcd (%) for C₄₈H₄₂Cl₂P₂Ru (852.12): C 67.60, H 4.96; found: C 67.82, H 5.25.

4.2.2. RuCl₂(3-iso-propyl-1-indenylidene)(PCy₃)₂, **7a**

(0.42 g, 95%). ¹H NMR (500 MHz, CDCl₃, 20 °C, TMS): δ 8.57 (d, ³J_{H,H} = 7.3 Hz, 1H, H-7), 7.30 (t, ³J_{H,H} = 7.3 Hz, 1H, H-5), 7.18–7.21 (m, 2H, H-2 and H-6), 6.95 (d, ³J_{H,H} = 7.0 Hz, 1H, H-4), 2.57–2.61 (m, 6H, H-PCy₃), 2.26 (sept, ³J_{H,H} = 6.7 Hz, 1H, H-10), 1.86–1.88 (m, 6H, H-PCy₃), 1.75 (s, 12H, H-PCy₃), 1.66 (s, 12H, H-PCy₃), 1.40–1.52 (m, 12H, H-PCy₃), 1.15–1.24 (m, 24H, H-11, H-PCy₃); ¹³C{¹H}NMR (126 MHz, CDCl₃, 20 °C): δ 297.8 (t, ²J_{C,P} = 7.6 Hz, C-1), 148.4 (C-3), 143.7 (C-8), 141.5 (C-9), 136.9 (C-2), 128.8 (C-7), 128.7 (C-6), 128.4 (C-5), 115.6 (C-4), 32.4–32.6 (C-PCy₃), 29.7–29.8 (C-PCy₃), 27.7–27.9 (C-PCy₃), 27.3 (C-10), 26.6 (C-PCy₃), 19.6 (C-11). ³¹P{¹H}NMR (203 MHz, CDCl₃, 20 °C): δ 31.4 (s). IR (Neat): ν = 2929, 2851, 1549, 1446, 1360, 1345, 1328, 1301, 1266, 1222, 1199, 1174, 1129, 1109, 1046, 1004, 918, 916, 888, 847, 767, 754, 733, 708 cm⁻¹; elemental analysis calcd (%) for C₄₈H₇₈Cl₂P₂Ru (888.40): C 64.85, H 8.84; found: C 64.78, H 8.92.

4.2.3. $\text{RuCl}_2(3\text{-tert-butyl-1-indenylidene})(\text{PPh}_3)_2$, **6b**

^1H NMR (300 MHz, CDCl_3 , 20 °C, TMS): δ 7.48–7.53 (m, 12H), 7.38 (t, $^3J_{\text{H,H}} = 7.2$ Hz, 6H), 7.27 (t, $^3J_{\text{H,H}} = 7.4$ Hz, 12H), 7.20 (t, $^3J_{\text{H,H}} = 7.4$ Hz, 1H), 7.09 (d, $^3J_{\text{H,H}} = 7.4$ Hz, 1H), 7.02 (d, $^3J_{\text{H,H}} = 7.2$ Hz, 1H), 6.49 (t, $^3J_{\text{H,H}} = 7.2$ Hz, 1H), 6.19 (s, 1H), 1.11 (s, 9H); $^{31}\text{P}\{\text{H}\}$ NMR (121 MHz, CDCl_3 , 20 °C): δ 29.1 (s); elemental analysis calcd (%) for $\text{C}_{49}\text{H}_{44}\text{Cl}_2\text{P}_2\text{Ru}$ (866.13): C 67.90, H 5.12; found: C 67.58, H 5.39.

4.2.4. $\text{RuCl}_2(3\text{-tert-butyl-1-indenylidene})(\text{PCy}_3)_2$, **7b**

(0.41 g, 91%). ^1H NMR (500 MHz, CDCl_3 , 20 °C, TMS): δ 8.58 (d, $^3J_{\text{H,H}} = 7.3$ Hz, 1H, H-7), 7.29 (t, $^3J_{\text{H,H}} = 7.3$ Hz, 1H, H-5), 7.15–7.19 (m, 3H, H-2, H-4 and H-6), 2.57–2.61 (m, 6H, H- PCy_3), 1.86–1.89 (m, 6H, H- PCy_3), 1.74–1.76 (m, 12H, H- PCy_3), 1.66 (s, 12H, H- PCy_3), 1.40–1.52 (m, 12H, H- PCy_3), 1.32 (s, 9H, H-11), 1.15–1.27 (m, 18H, H- PCy_3); $^{13}\text{C}\{\text{H}\}$ NMR (126 MHz, CDCl_3 , 20 °C): δ 298.0 (t, $^2J_{\text{C,P}} = 7.6$ Hz, C-1), 149.3 (C-3), 144.8 (C-8), 140.3 (C-9), 137.5 (C-2), 128.9 (C-7), 128.2 (C-5), 128.1 (C-6), 118.7 (C-4), 33.9 (C-10), 32.6–32.7 (C- PCy_3), 29.8–29.9 (C- PCy_3), 27.7–28.0 (C- PCy_3), 27.7 (C-11), 26.6 (C- PCy_3). $^{31}\text{P}\{\text{H}\}$ NMR (202 MHz, CDCl_3 , 20 °C): δ 31.3 (s). IR (Neat): $\nu = 2910, 2854, 1541, 1447, 1364, 1346, 1329, 1301, 1259, 1198, 1183, 1175, 1129, 1110, 1004, 915, 896, 887, 848, 768, 754, 732 \text{ cm}^{-1}$; elemental analysis calcd (%) for $\text{C}_{49}\text{H}_{80}\text{Cl}_2\text{P}_2\text{Ru}$ (902.42): C 65.17, H 8.93; found: C 65.49, H 8.88.

4.2.5. $\text{RuCl}_2(3\text{-cyclohexyl-1-indenylidene})(\text{PPh}_3)_2$, **6c**

^1H NMR (300 MHz, CDCl_3 , 20 °C, TMS): δ 7.48–7.53 (m, 12H), 7.38 (t, $^3J_{\text{H,H}} = 7.4$ Hz, 6H), 7.27 (t, $^3J_{\text{H,H}} = 7.4$ Hz, 12H), 7.19 (t, $^3J_{\text{H,H}} = 7.5$ Hz, 1H), 6.93 (d, $^3J_{\text{H,H}} = 6.8$ Hz, 1H), 6.85 (d, $^3J_{\text{H,H}} = 7.2$ Hz, 1H), 6.52 (t, $^3J_{\text{H,H}} = 7.4$ Hz, 1H), 6.15 (s, 1H), 1.70–1.81 (m, 6H), 0.98–1.39 (m, 5H); $^{31}\text{P}\{\text{H}\}$ NMR (121 MHz, CDCl_3 , 20 °C): δ 29.5 (s); elemental analysis calcd (%) for $\text{C}_{51}\text{H}_{46}\text{Cl}_2\text{P}_2\text{Ru}$ (892.15): C 68.61, H 5.19; found: C 68.90, H 5.05.

4.2.6. $\text{RuCl}_2(3\text{-cyclohexyl-1-indenylidene})(\text{PCy}_3)_2$, **7c**

(0.43 g, 93%). ^1H NMR (500 MHz, CDCl_3 , 20 °C, TMS): δ 8.57 (d, $^3J_{\text{H,H}} = 7.3$ Hz, 1H, H-7), 7.29 (t, $^3J_{\text{H,H}} = 7.3$ Hz, 1H, H-5), 7.19 (t, $^3J_{\text{H,H}} = 7.6$ Hz, 1H, H-6), 1H, 7.13 (s, 1H, H-2), 6.94 (d, $^3J_{\text{H,H}} = 7.3$ Hz, 1H, H-4), cyclohexyl signals: 2.59, 1.98, 1.94, 1.88, 1.81, 1.74, 1.65, 1.37–1.52, 1.15–1.24; $^{13}\text{C}\{\text{H}\}$ NMR (126 MHz, CDCl_3 , 20 °C): δ 298.0 (t, $^2J_{\text{C,P}} = 7.6$ Hz, C-1), 147.3 (C-3), 143.6 (C-8), 141.5 (C-9), 137.4 (C-2), 128.8 (C-7), 128.6 (C-6), 128.3 (C-5), 115.5 (C-4), cyclohexyl signals: 37.3 (C-10), 32.5, 30.1, 29.8, 27.8, 26.6, 26.4. $^{31}\text{P}\{\text{H}\}$ NMR (202 MHz, CDCl_3 , 20 °C): δ 31.5 (s). IR (Neat): $\nu = 2930, 2854, 1547, 1446, 1346, 1328, 1301, 1295, 1270, 1230, 1205, 1198, 1175, 1130, 1110, 1077, 1020, 1004, 942, 916, 897, 888, 848, 753, 732 \text{ cm}^{-1}$; elemental analysis calcd (%) for $\text{C}_{51}\text{H}_{82}\text{Cl}_2\text{P}_2\text{Ru}$ (928.43): C 65.93, H 8.90; found: C 65.79, H 8.95.

Acknowledgements

F.V. would like to express his deep appreciation to the State Key Lab of Advanced Technology for Materials Synthesis and Processing for financial support (Wuhan University of Technology). F.V. acknowledges the Chinese Central Government for an Expert of the State position in the program of Thousand Talents and the support of the Natural Science Foundation of China (No. 21172027). B.Y. and F.V. appreciate the Research Fund – Flanders (FWO) (project No. 3G022912) for funding. K.V.H. thanks the Hercules Foundation (project AUGE/11/029 "3D-SPACE: 3D Structural Platform Aiming for Chemical Excellence") and the Research Fund - Flanders (FWO) for funding. K.L. acknowledges the Special Research Fund of Ghent University for a postdoctoral grant (No. 01P06813T).

Appendix A. Supplementary data

Supplementary data related to this article can be found at <http://dx.doi.org/10.1016/j.jorgchem.2015.04.054>.

References

- [1] (a) A. Fürstner, Angew. Chem. 112 (2000) 3140–3172. Angew. Chem. Int. Ed. 39 (2000) 3012–3043;
- (b) T.M. Trnka, R.H. Grubbs, Acc. Chem. Res. 34 (2001) 18–29;
- (c), in: R.H. Grubbs (Ed.), Handbook of Metathesis, vol. 1–3, Wiley-VCH, Weinheim, 2003, 1–1234;
- (d) D. Astruc, New. J. Chem. 29 (2005) 42–56;
- (e) P.H. Deshmukh, S. Blechert, Dalton Trans. (2007) 2479–2491.
- [2] S.T. Nguyen, L.K. Johnson, R.H. Grubbs, J.W. Ziller, J. Am. Chem. Soc. 114 (1992) 3974–3975.
- [3] (a) P. Schwab, M.B. France, J.W. Ziller, R.H. Grubbs, Angew. Chem. 107 (1995) 2179–2181. Angew. Chem. Int. Ed. Engl. 34 (1995) 2039–2041;
- (b) P. Schwab, R.H. Grubbs, J.W. Ziller, J. Am. Chem. Soc. 118 (1996) 100–110;
- (c) E.L. Dias, S.T. Nguyen, R.H. Grubbs, J. Am. Chem. Soc. 119 (1997) 3887–3897.
- [4] (a) L. Ackermann, A. Fürstner, T. Weskamp, F.J. Kohl, W.A. Herrmann, Tetrahedron Lett. 40 (1999) 4787–4790;
- (b) M. Scholl, S. Ding, C.W. Lee, R.H. Grubbs, Org. Lett. 1 (1999) 953–956;
- (c) M. Scholl, T.M. Trnka, J.P. Morgan, R.H. Grubbs, Tetrahedron Lett. 40 (1999) 2247–2250;
- (d) J. Huang, E.D. Stevens, S.P. Nolan, J.L. Petersen, J. Am. Chem. Soc. 121 (1999) 2674–2678.
- [5] (a) J.S. Kingsbury, J.P. Harrity, P.J. Bonitatebus, A.H. Hoveyda, J. Am. Chem. Soc. 121 (1999) 791–799;
- (b) M.R. Buchmeiser, Chem. Rev. 100 (2000) 1565–1604.
- [6] (a) L.Jafarpour, H.J. Schanz, E.D. Stevens, S.P. Nolan, Organometallics 18 (1999) 5416–5419;
- (b) A. Fürstner, M. Liebl, A.F. Hill, J.D. Wilton-Ely, Chem. Commun. (1999) 601–602;
- (c) A.M. Lozano-Vila, S. Monsaert, A. Bajek, F. Verpoort, Chem. Rev. 110 (2010) 4865–4909.
- [7] (a) A. Fürstner, O. Guth, A. Düffels, G. Seidel, M. Liebl, B. Gabor, R. Mynott, Chem. Eur. J. 7 (2001) 4811–4820;
- (b) E.A. Shaffer, C.L. Chen, A.M. Beatty, E.J. Valente, H.J. Schanz, J. Organomet. Chem. 692 (2007) 5221–5233.
- [8] C. Samojlowicz, M. Bieniek, A. Pazio, A. Makal, K. Woźniak, A. Poater, L. Cavallo, J. Wójcik, K. Zdanowski, K. Grela, Chem. Eur. J. 17 (2011) 12981–12993.
- [9] R. Dorta, R.A. Kelly, S.P. Nolan, Adv. Synth. Catal. 346 (2004) 917–920.
- [10] (a) S. Randl, S. Gessler, H. Wakamatsu, S. Blechert, Synlett 3 (2001) 430–432;
- (b) H. Clavier, S.P. Nolan, M. Mauduit, Organometallics 27 (2008) 2287–2292;
- (c) A. Kirschning, Ł. Gutajski, K. Mennecke, A. Meyer, T. Busch, K. Grela, Synlett 17 (2008) 2692–2696;
- (d) E. Borré, F. Caijo, C. Crévisy, M. Mauduit, Beilstein J. Org. Chem. 6 (2010) 1159–1166.
- [11] A. Kabro, T. Roisnel, C. Fischmeister, C. Bruneau, Chem. Eur. J. 16 (2010) 12255–12261.
- [12] A. Kabro, G. Ghattas, T. Roisnel, C. Fischmeister, C. Bruneau, Dalton Trans. 41 (2012) 3695–3700.
- [13] (a) L.R. Jimenez, B.J. Gallon, Y. Schrödi, Organometallics 29 (2010) 3471–3473;
- (b) L.R. Jimenez, D.R. Tolentino, B.J. Gallon, Y. Schrödi, Molecules 17 (2012) 5675–5689.
- [14] B. Yu, Y. Xie, F.B. Hamad, K. Leus, A.A. Lyapkov, K. Van Hecke, F. Verpoort, New. J. Chem. 39 (2015) 1858–1867.
- [15] (a) F. Boeda, H. Clavier, S.P. Nolan, Chem. Commun. (2008) 2726–2740;
- (b) A.M. Lozano-Vila, S. Monsaert, A. Bajek, F. Verpoort, Chem. Rev. 110 (2010) 4865–4909.
- [16] (a) R. Castarlenas, C. Vovard, C. Fischmeister, P.H. Dixneuf, J. Am. Chem. Soc. 128 (2006) 4079–4089;
- (b) T. Opstal, F. Verpoort, J. Mol. Catal. A-Chem. 200 (2003) 49–61;
- (c) N. Ledoux, R. Drozdak, B. Allaert, A. Linden, P. Van Der Voort, F. Verpoort, Dalton Trans. 44 (2007) 5201–5210.
- [17] D.M. Hudson, E.J. Valente, J. Schachner, M. Limbach, K. Müller, H.J. Schanz, ChemCatChem 3 (2011) 297–301.
- [18] M. Lichtenheldt, S. Kress, S. Blechert, Molecules 17 (2012) 5177–5186.
- [19] K. Harlow, A. Hill, J.E. Wilton-Ely, J. Chem. Soc. Dalton Trans. (1999) 285–292.
- [20] Some reviews see: (a) M.I. Bruce, Chem. Rev. 98 (1998) 2797–2858;
- (b) V. Cadierno, M.P. Gamasa, J. Gimeno, Eur. J. Inorg. Chem. (2001) 571–591;
- (c) R. Castarlenas, C. Fischmeister, C. Bruneau, P.H. Dixneuf, J. Mol. Catal. A: Chem. 213 (2004) 31–37;
- (d) R.F. Winter, S. Záliš, Coord. Chem. Rev. 248 (2004) 1565–1583;
- (e) S. Rigaut, D. Touchard, P.H. Dixneuf, Coord. Chem. Rev. 248 (2004) 1585–1601;
- (f) C.M. Che, C.M. Ho, J.S. Huang, Coord. Chem. Rev. 251 (2007) 2145–2166;
- (g) K. Ofele, E. Tosh, C. Taubmann, W. Herrmann, Chem. Rev. 109 (2009) 3408–3444;
- (h) V. Cadierno, J. Gimeno, Chem. Rev. 109 (2009) 3512–3560.
- [21] (a) C. Bianchini, M. Peruzzini, F. Zanobini, C. Lopez, I. de los Rios, A. Romerosa,

- Chem. Commun. (1999) 443–444;
(b) E.S. Ma, B.O. Patrick, B.R. James, Inorg. Chim. Acta 408 (2013) 126–130.
- [22] P.L. Chiu, H.M. Lee, Organometallics 24 (2005) 1692–1702.
- [23] E.A. Shapiro, A.V. Kalinin, B.I. Ugrak, O.M. Nefedov, J. Chem. Soc. Perkin Trans. 2 (1994) 709–713.
- [24] R.W. Saalfrank, A. Welch, M. Haubner, U. Bauer, Liebigs Annalen 2 (1996) 171–181.
- [25] M. Hatano, T. Mizuno, K. Ishihara, Tetrahedron 67 (2011) 4417–4424.
- [26] R. Winde, R. Karch, A. Rivas-Nass, A. Doppiu, G. Peter, E. Woerner, US Pat. 0190524 A1 (2011).
- [27] D.R. Lane, C.M. Beavers, M.M. Olmstead, N.E. Schore, Organometallics 28 (2009) 6789–6797.
- [28] C.A. Urbina-Blanco, A. Poater, T. Lebl, S. Manzini, A.M. Slawin, L. Cavallo, S.P. Nolan, J. Am. Chem. Soc. 135 (2013) 7073–7079.
- [29] T. Ritter, A. Hejl, A.G. Wenzel, T.W. Funk, R.H. Grubbs, Organometallics 25 (2006) 5740–5745.
- [30] S. Monsaert, R. Drozdak, V. Dragutan, I. Dragutan, F. Verpoort, Eur. J. Inorg. Chem. (2008) 432–440.
- [31] M. Zaja, S.J. Connolly, A.M. Dunne, M. Rivard, N. Buschmann, J. Jiricek, S. Blechert, Tetrahedron 59 (2003) 6545–6558.
- [32] (a) H. Clavier, C.A. Urbina-Blanco, S.P. Nolan, Organometallics 28 (2009) 2848–2854;
(b) S. Manzini, C.S.A. Urbina Blanco, A.M. Slawin, S.P. Nolan, Organometallics 31 (2012) 6514–6517.
- [33] (a) M.S. Sanford, J.A. Love, R.H. Grubbs, Organometallics 20 (2001) 5314–5318;
(b) J.A. Love, M.S. Sanford, M.W. Day, R.H. Grubbs, J. Am. Chem. Soc. 125 (2003) 10103–10109;
(c) X. Sauvage, G. Zaragoza, A. Demonceau, L. Delaude, Adv. Synth. Catal. 352 (2010) 1934–1948.
- [34] A.P. Shaw, B.L. Ryland, J.R. Norton, D. Buccella, A. Moscatelli, Inorg. Chem. 46 (2007) 5805–5812.
- [35] H. Clavier, S.P. Nolan, Chem. Eur. J. 13 (2007) 8029–8036.
- [36] CrysAlisPro, Agilent Technologies, Version 1.171.36.28.
- [37] O.V. Dolomanov, L.J. Bourhis, R.J. Gildea, J.A.K. Howard, H. Puschmann, J. Appl. Cryst. 42 (2009) 339–341.
- [38] SHELXS G.M. Sheldrick, Acta Cryst. A64 (2008) 112–122.
- [39] SHELXL G.M. Sheldrick, Acta Cryst. A64 (2008) 112–122.